## IMECE2021-73138

# STRUCTURE AND MEASUREMENT OF ATMOSPHERIC AND HIGH-PRESSURE IGNITION PLASMA

James Shaffer West Virginia University Morgantown, WV Saeid Zare Mississippi State University Starkville, MS Omid Askari West Virginia University Morgantown, WV

#### **ABSTRACT**

Experiments are conducted to understand atmospheric spark ignition process in more detail. The research done relates the electrical energy dissipated across the spark gap to the measured schlieren ignition volume. The result is the supplied electrical thermal energy. The study provides insight into the structure of plasma and the mechanisms which convert electrical power into heat. The research is done to support laminar burning speed calculations to increase accuracy and extend diagnostic techniques to conditions otherwise immeasurable. Typically, plasma measurements are taken via a Langmuir probe. However, for the automotive ignition plasma, this measurement technique is challenging because of the transient nature, high pressure, and temperatures involved. Therefore, several alternative techniques will be used in order to find the potential distribution of the plasma and unveil the structure of the plasma more specifically the cathode fall. Three different voltage measurements are taken in order to capture the cathode fall of the plasma. One method simply measures the potential using a high voltage probe. This method may be inaccurate because of the presence of charged ions, however, these results are compared to non-intrusive measurements where voltage data is extrapolated over various gaps sizes to zero length. It is generally agreed that the desired measurement for this work, the cathode fall, remain constant and depends on the composition of the gas and the electrode. Therefore, changing the system input power and the gap will only change the voltage drop across the bulk plasma. The linear change in voltage potential through variation of testing parameters like gap length can then be extrapolated to zero length of the bulk plasma or minimum energy value which should be equal the value of cathode fall and bulk plasma potential respectively. It was found that after excluding systemic losses such as electrical resistance and ignition coil inefficiencies, the primary loss within the plasma gap is the potential drop across the cathode sheath. Excluding the loss in the cathode fall results in a measured electrical data that is responsible for thermal discharge. In order to highlight the findings, electrical discharge energy is compared to the volume of the heated gas kernel in atmospheric air. Removal of the cathode fall data will show that the energy is proportional to the volume of heated gas whereas, before the change in energy dissipation between glow and arc plasmas prevented this relationship from being visible. The data and methods discussed in this research provides the means to determine the thermal energy of ignitions and sparks even when the spark is inaccessible or obscured. Further work will be done utilizing the power measurement found in this work in a model to predict the affected thermal spark volume. It is also proposed that further validation of the proposed measured electrical thermal energy should be compared to the energy measured with a calorimeter to determine any other inefficiencies in the plasma discharge process. Additionally, the experimentation done observes the cathode fall of only glow plasma, Additional work should be done to find the cathode fall of arc plasma.

Keywords: Ignition, Glow Plasma, Arc plasma, DC plasma discharge, Atmospheric Plasma, Combustion, Thermodynamics, Measurement techniques

## 1. INTRODUCTION

First, the current model of electrical plasma should be explored. A thorough understanding of the fundamental processes begins with Irving Langmuir's initial work with low pressure plasmas. Experiments utilizing mercury rectifiers provided one of the first indication of what occurs physically within the discharge event [1]. Langmuir was able to show and describe sheath formation with measurements taken via a biased probe. Ionization within the plasma produces positive ions that can react to and affect electric field within the spark gap. A detailed mathematical explanation of the motion of the charged particles between the plasma electrodes has been considered and studied in many works over many years. The work has resulted in

electric field descriptions that show the formation of thin sheaths at the surface of the electrode. A generalized illustration of sheath formation for DC plasma is shown in Fig. 1. The motion of the heavy positive ions to form the sheath is the result of high electric fields near the charged electrode. The highly negative charge of the cathode strongly attracts the positive ions whereas the anode's ground potential compared to the positively charged bulk plasma will weakly attract the positive ions causing a weak field increase at the ground electrode and a slightly higher density.

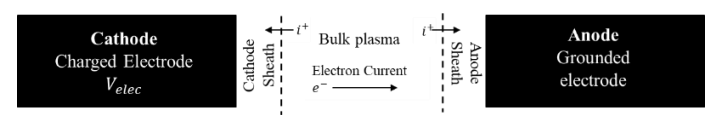


FIGURE 1: MODEL OF THE DC PLASMA.

Typically for DC cases the anode sheath is considered to be small or negligible since the electrode is neutral and would not have the same intense electric field as the charged electrode. Because of the importance in the thermal energy description, this work will consider the affect an anode sheath will have on the measurement. The detailed work and relations that can describe the formation and motion of these sheaths can be found in Tonks and Langmuir, as well as Lieberman's works [2,3]. For the atmospheric plasma discharge explored in this work, it is also important to understand the discharge regimes available to the operating pressures.

There are three major events that can occur during an atmospheric spark discharge. The first is the breakdown event which is extremely short lived on the order of nanosecond. The peak power is intense and causes a moment of fully ionized gas at high temperature (>10000K). The breakdown is largely an efficient process but can supply very little energy (on the order of <1 mJ, depending on the experimental conditions) to the ignition kernel so it will not be explored in detail in this work. Once the breakdown ends, the partially recombined gas then partakes in either arc or glow discharge. The arc discharge is characterized by a lower voltage on the order of 50V-100V with larger current measurements. The glow discharge is characterized with a high voltage (~500V) and low current. Both of these plasma events should produce some physical sheath at the surface of the electrode as a boundary between the electrode and plasma. Additional models can describe the physics of the formations within the plasma for both glow [4– 11] and arc[12–15]. A detailed analysis of both arc and glow mode sheath formation is certainly interesting and useful; however the level of detail is considered excessive for the goals of the present work. On a macroscopic scale where the plasma is considered in equilibrium, a simplified model is considered. It is proposed that a majority of the non-thermal losses measured within plasma gap can be captured by considering only the glow mode cathode sheath. There may be more losses within the arc phase sheath formation, but these losses will be far smaller because of the reduced voltage and field causing a much smaller sheath (in terms of electrode surface area) to

form. The small size of the sheath results in a smaller energy dissipation across this region when compared to glow discharge. Neglecting sheath formation in the arc phase is acceptable as some models consider no sheath formation to occur as discussed by Benilov et al. [12].

Further, it is important to discuss the evidence of total non-thermal loss resulting from the sheath formation. The work from Ziegler et al [16] shows that despite consistent composition the minimum ignition energy increases with an increase in cathode fall voltage. This suggests that the cathode fall is truly non thermal and can be neglected. The explanation for this loss of voltage can be found in the thickness of the sheath at these pressures. First, an approximation of the cathode fall,  $V_n$ , and thickness,  $d_n$ , can be found for normal glow using Eqs. 1 and 2 [17],

$$V_n = \frac{^{3B}}{^A} ln \left( 1 + \frac{1}{\gamma} \right) \tag{1}$$

$$d_n p = 0.82 \frac{\ln\left(1 + \frac{1}{\gamma}\right)}{A} \tag{2}$$

A=14.6 and B=365 are constants found for the specific gas related to the electron ionization coefficient.  $\gamma$  represents the electrons emitted from the electrode for every positive ion impact. A value of 0.02 was used for iron electrode in air. These relations predict a cathode fall for iron in air to be 295V. The experimentally found fall reported in Cobine is 269V [17]. The value of cathode fall is considered to be constant regardless of the supplied electrical current but can change for variations in electrode and gas compositions. The work here considers stainless steel wire electrodes which should be similar in magnitude to the theoretical and measured data in Cobine but is likely different in practice.

The estimated cathode fall thickness and the free mean path for the atmospheric plasma is on the order of nanometers. With the fall thickness and free mean path so close in magnitude the region which is responsible for the cathode fall is largely collision-less resulting in a non-thermal sheath. The defining characteristic of normal glow results from the current density (the electron current divided by the cathode surface area) that arises for the given pressure to have the minimum cathode fall voltage. The cathode fall will become elevated should the current density increase. If the cathode surface is larger than the size of the plasma then any glow observed should be in the normal state. The theoretical current density is given by Eq. 3 [17],

$$j_n = 5.95 * 10^{-14} \frac{AB^2 K_p p(1+\gamma)B^2}{\ln\left(1+\frac{1}{\gamma}\right)}$$
 (3)

where  $K_p$  is the mobility of the positive ions. A value of 1.36 is used for this estimate. Pressure is in mmHg and current density is in amp per  $cm^2$ . The estimate shows that for an electrode wire diameter of 0.25mm the predicted current and electrode sheath coverage is similar to what is seen experimentally in Fig. 2.

The expected growth predicted theoretically is also plotted in Fig. 2 using Eq. 3. The data is plotted up to 0.6 amps and the predicted sheath growth is on the same order as the experimental results. Figure 3 illustrates the typical data for the system used in this work to explicitly define which data are in arc and glow phase. The change between arc and glow discharge is signified by a sudden shift in voltage where the glow discharge is the high voltage discharge. The glow plasma obtained experimentally is considered to be in normal glow since the surface of the electrode is not restricted. We should next see how this manifest in the actual experimental conditions.

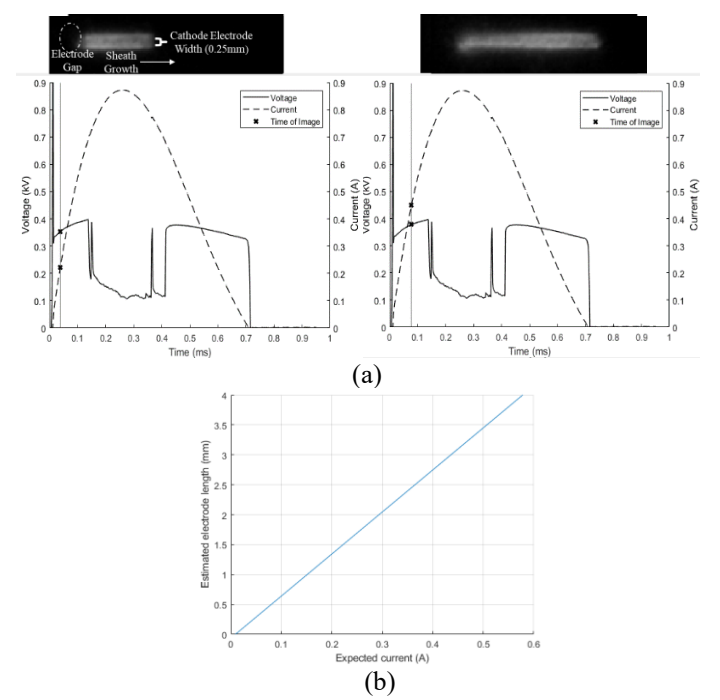
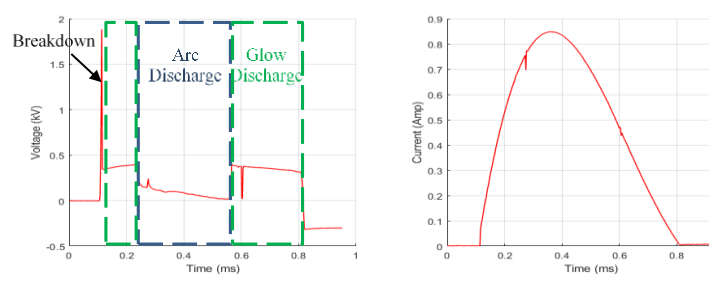
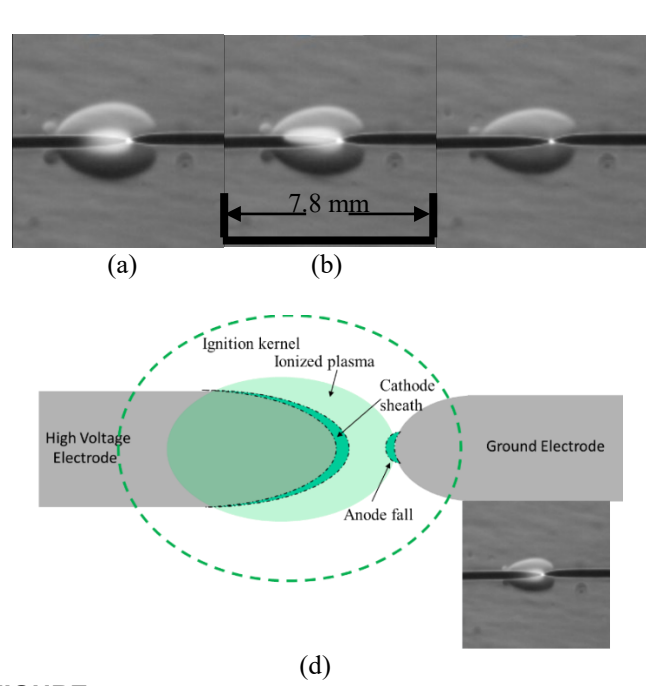


FIGURE 2: (a) EXPERIMENTALLY OBSERVED SHEATH GROWTH ALONG ELECTRODE VISUALIZED WITH CHEMILUMINESCENT INTENSITY IMAGES AND PLOTTED WITH THE VOLTAGE AND CURRENT, IMAGE TIME INDICATED WITH VERTICAL LINE; (b) PLOT OF EXPECTED CURRENT TO SHEATH LENGTH.



**FIGURE 3:** SAMPLE VOLTAGE AND CURRENT DATA WITH IDENTIFICATION OF ARC AND GLOW MODES.

Figure 4 uses a sample case with a mixture of Nitrogen and Methane to highlight the difference between the plasma region and the low-density heated kernel shown via the Schlieren technique. One can see that the glow discharge is indeed a volumetric discharge that occurs over a large area of the high voltage electrode (left) as described in Eq. 3 and shown in Fig. 2. Arc shown in Fig. 4b and Fig. 4c is a point-to-point discharge that can occur anywhere on the electrode which can result in very noisy non-uniform visual data. For this reason, it is desired to have full glow discharge for all data as the kernels are symmetric and smooth resulting in good measurable data. In theory, all plasma should be in glow discharge if the electrode has a large enough surface area to meet the normal glow discharge current density requirements; however, for real systems many factors come into play which can cause arc discharge. If the electrode surface is rough or dirty, arc will form, especially at high pressures and current. If glow discharge is desired at high pressures, an extremely smooth and clean electrode should be maintained.



**FIGURE 4:** KERNEL AND BRIGHT PLASMA REGION OF (a) GLOW DISCHARGE (b) SURFACE POINT TO TIP ARC DISCHARGE, (c) TIP TO TIP ARC DISCHARGE AND (d) DIAGRAM OF GLOW DISCHARGE

A drawing is also presented in Fig. 4 to illustrate the shape and structure of the experimental glow plasma more clearly. The actual sheath formation is not visible experimentally because of its small size. For the results, in this work, the effect that the transient nature of the spark has on the measurement should be considered. For large gaps or pressures the plasma requires greater voltages to initially ionize the region. After some time, the voltage will settle to the steady state value. Cobine [17] discusses this in his work and consequently measurements

taken should be selected carefully and not measured within the start and end of the spark to prevent erroneous measurements.

The majority of the analysis on the data will consider a zero length extrapolation as detailed by Hao et al [18]. Part of the assumption with this extrapolation is that the electric field within the bulk plasma is constant or as a constant drop in potential. This would make the region ohmic in nature so for every change in gap length a proportional voltage change will occur in the data. This method will be expanded by considering smaller gaps than examined in Hao's work and by considering current change at constant gaps and floating probe voltage measurements as alternate methods.

## 2. MATERIALS AND METHODS

## 2.1 Spark Generation and Measurement

The circuit provided in Fig. 5 produces a high voltage pulse to the spark gap by passing a high current pulse through the primary windings of the ignition coil. The result is sinusoidal current shape driven by the second order LCR circuit similar referenced patent [19]. By changing the initial stored voltage in the capacitor, the magnitude of the current passed is changed. The secondary coil will see a current pulse on the order of 1 amp. The duration of the pulse is driven by the inductance and resistance of the ignition coil, a street fire 5527 automotive coil.

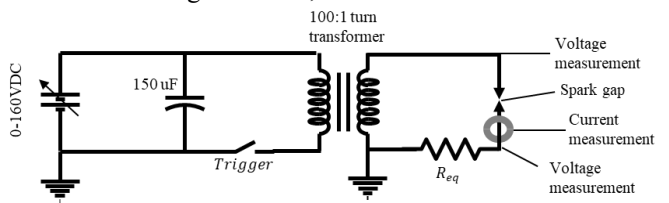


FIGURE 5: SIMPLIFIED CIRCUIT DIAGRAM OF IGNITION SYSTEM AND MEASUREMENT PROBE LOCATIONS

The voltage is captured using a Northstar PVM-4 probe which has a 0.4% uncertainty and the current is captured using a Pearson 6595 Current monitor which has a 1% uncertainty. The probe measurements are then captured using an NI-9222 four channel ADC which has 16 bits of vertical resolution and a sample rate of 500k. The uncertainty was captured using standard uncertainty techniques. The coil measurement is affected by droop which causes the actual value of current to reduce over time. This is corrected for by using Eq. 4, and is demonstrated in Fig. 6a

$$i_{Correct} = i_{Meas} + \frac{\int i_{Meas}}{\tau} \tag{4}$$

The voltage and current data captured is used to find power and energy which is found using Eqs. 5 and 6.

$$P(t)_{elec} = V(t) * I(t)$$
(5)

$$P(t)_{elec} = V(t) * I(t)$$
 (5)  
 
$$E(t)_{elec} = \int P(t) dt, E_{Total} = \int_{t_1}^{t_2} P(t) dt$$
 (6)

A sample of this data is provided in Fig. 6. The data also includes error bars on every 10th data point to show the expected uncertainty in the data.

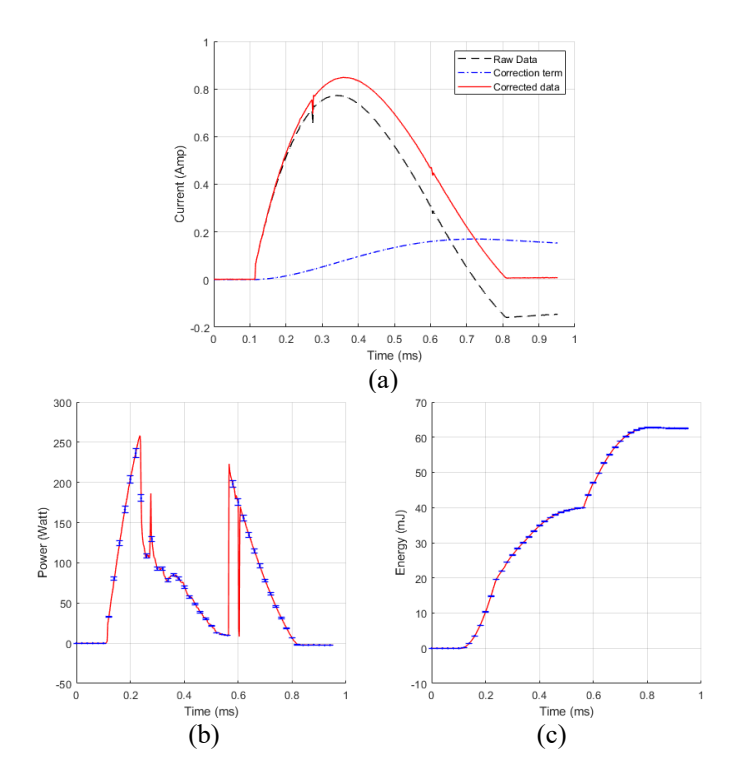


FIGURE 6: (a) CURRENT MEASUREMENT INDUCTIVE DROOP CORRECTION, (b) POWER AND (c) ENERGY MEASUREMENTS WITH UNCERTAINTY.

## 2.2 Visual Images and Measurement

Schlieren images are captured with a Toepler type setup utilizing two Plano-convex lenses in a linear formation [20]. A Phantom V611 is used to capture the images. Typical setting use a 128x128 pixel window with a 180k fps sample rate. The camera lens is a sigma DG 300mm model and is capable of imaging the spark kernel with a resolution on the scale in the range of 10-23 px/mm, depending on the specific settings. The lighting system is a Thorlabs 700mW, 625nm wavelength LED light. A system schematic is shown in Fig. 7.

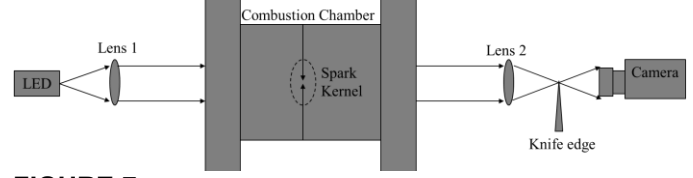


FIGURE 7: SCHLIEREN SETUP.

The combustion chamber is cylindrical and has a diameter and height of 5.25 inches and uses borosilicate glasses to provide visual access to the ignition kernel. A knife cuts the light at the focal point of the second lens to provide the Schlieren effect. A more detailed look at the kernel size measurement is done in a separate work as this work only utilizes the final kernel volume for a brief comparison.

## 2.3 Experiments

The results captured will evaluate three different techniques for measuring the cathode fall of the plasma and how the voltage drops across each structure of the discharge. The first technique will simply take floating voltage measurements of the plasma itself across a 1mm gap utilizing a probe. Three measurements will be taken to show how the voltage drops across the bulk plasma. The second method shown will vary the size of the gap to see the change in measured voltage which will then be extrapolated to zero length to eliminate all ohmic voltage drops. The third method changes the magnitude of the current passed through a constant gap which also should highlight the ohmic voltage drops within the plasma. A table of testing parameters are shown in Table 1.

**TABLE 1:** EXPERIMENTAL PARAMETERS PRESENTED IN THIS WORK

Test type	Initial Stored Voltage	Electrode Thickness/ gap	Material/ Composition
Probe	130V	0.5 mm/	304 SS/
Measurements		1mm	air
Gap Change	130V	0.5 mm/	304 SS/
Measurements		0.06 - 4.5mm	air
Voltage Change	50-160V	0.5 mm/	304 SS/
Measurements		1mm	Air
Energy-Volume	50-160V	0.5 mm/	304 SS/
Comparison		~0.05 mm	Air

## 3. RESULTS AND DISCUSSION

## 3.1 Probe Measurements

The voltage measurements over time for 3 discharge events where the voltage measurement probe is moved in relation to the high voltage electrode are shown in Fig. 8a. The placement of the measuring probe for each discharge is shown in the schlieren image seen as the vertical black line. Figure 8b then shows the voltage measurement against the spatial distance from the high voltage electrode in order to show the extrapolation to approximate the voltage at the boundary between the sheath and bulk plasma. The measurements show a small drop over the majority of the space with a large drop at the cathode and a smaller potential drop at the anode. The measurements appear to make a good estimation of the voltage drop however the effect of the positive ions within the plasma should be considered requiring further investigation. It should also be noted that the electrode surface condition is extremely important to the measurement of the cathode fall. In preliminary testing the cathode fall was measured around 230V while here it is 100V higher. It is believed that the actual value of the cathode fall can change not only with material but also

with shape as rough and sharp features on the electrode can affect the electric field that forms the sheath.

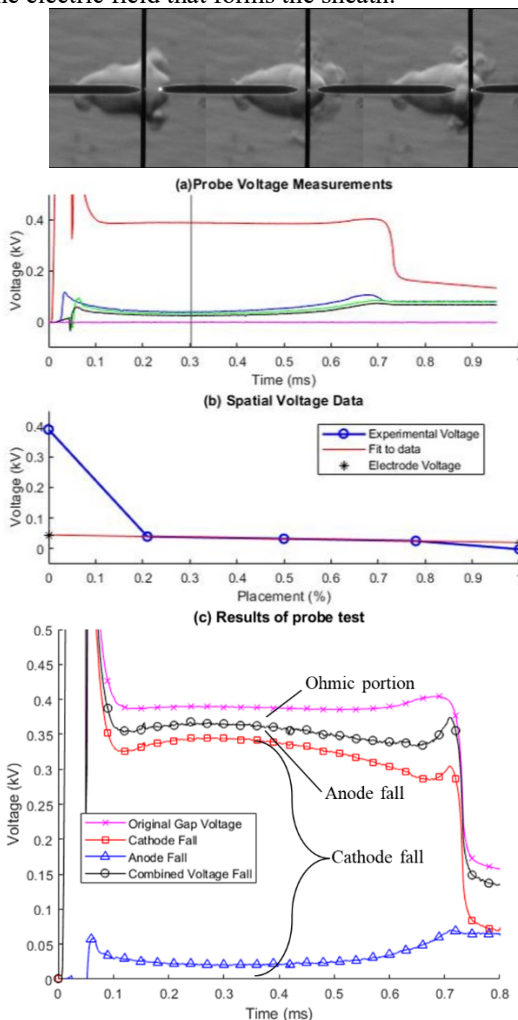


**FIGURE 8:** (a) PROBE SPATIAL MEASUREMENT, (b) EXTRAPOLATION RESULTS AT T=0.3MS AND (c) EXTRAPOLATION OVER ALL TIME.

The measured cathode and anode fall over time is also given in Fig. 8c with the original gap voltage as well as the combined fall voltages. The values of cathode and anode fall are taken at the time between 0.3 and 0.4 ms where the measurement is least affected by frequency and pressure affects. The measurements seem too give a good estimate of cathode fall when considering the magnitudes compared to other works and provides a visualization of how energy is dissipated across the physical structures of the plasma with the cathode sheath consuming a majority of the energy. This measurement will be compared to the zero length extrapolation in the next section.

### 3.2 Gap Change Measurements

The gap change tests consider the zero length extrapolation of the gap voltage as the gap length is changed. A sampling of the spark images is given in Figure 9. Here one can also see the effect of breakdown where large gaps produce a toroid shape from higher breakdown energies. The voltage data and example of the extrapolation is also shown Fig. 9. Here one can see that for very small gaps the measured gap voltage is almost exactly the same as the extrapolated value. For these results, it was hypothesized initially that for small gaps the measured extrapolation would be equal to the combined cathode and anode fall and at large gaps the anode fall would be small resulting in an extrapolation that measures closer to only the cathode fall. This was not the case even for large gaps the anode fall still has a large effect and should be considered present.

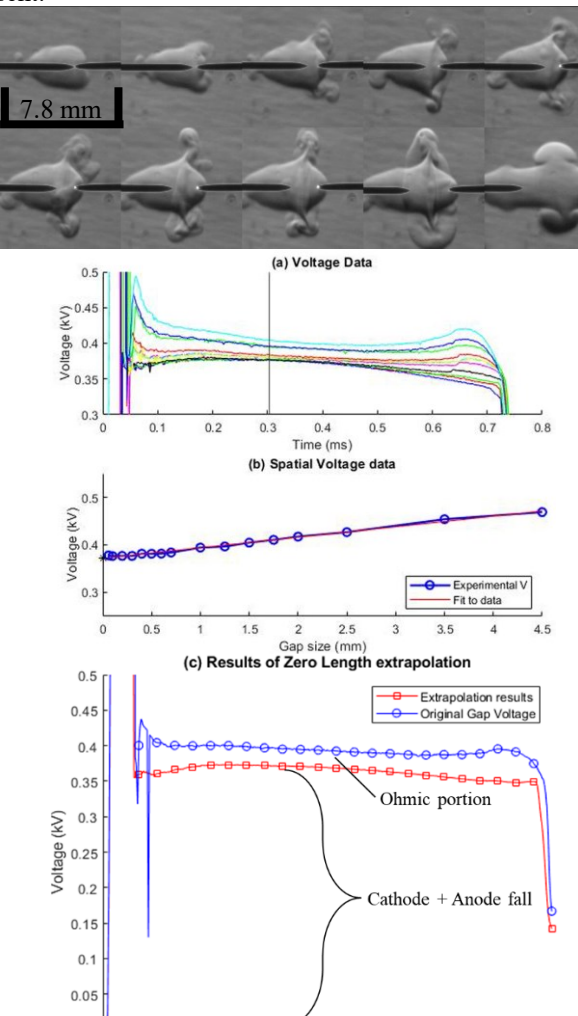


**FIGURE 9:** (a) ALL GAP CHANGE VOLTAGE DATA, (b) EXTRAPOLATION AT T=0.3MS AND (c) EXTRAPOLATION OVER ALL TIME.

The extrapolated data is also given over all time. Just as in the probe measurement the most accurate data should be taken when the transient start and finish of the spark is not affecting the data. The measured value is around  $370V \pm 10V$  which is close to the measured value of the combined cathode and anode fall measured with the probe, which is around  $365V \pm 10V$ . The

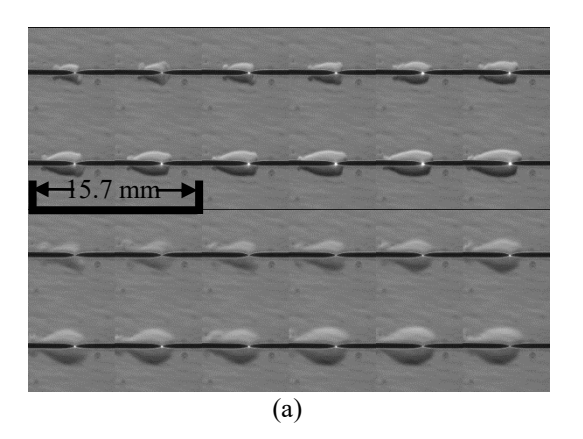
difference in the measurement could be the effect of the positive ions but this will be discussed in the concluding remarks.

## 3.3 Voltage Change Measurements

It was found that for a constant gap, increasing the initial stored voltage (increasing the magnitude of supplied current) did not cause a change in gap voltage for the Glow discharge. Since the radial direction from the electrode is not constrained as it is for the gap length the plasma kernel is able to expand and contract to accommodate the changing current. This means for a higher current, ionization will occur over a larger radial space, maintaining the voltage drop over this bulk plasma. Change with gap is observed because the length of the gap changes the minimum voltage requirement of the plasma. Therefore, no meaningful results were able to be capture through the analysis of changing current through the plasma

## 3.4 Energy-Radius Analysis

The final energy, with and without cathode fall, is compared to the final kernel volume to make an initial assessment of the measured cathode fall. Fig. 10 shows the final kernel images for the test as well as the energy and volume results. Ultimately, the chance that arc discharge occurs is partially random, and it occurred during the 9th and 12th test. Despite glow mode being extremely inefficient as compared to arc, Glow still typically outputs more thermal energy because of the significantly greater plasma volume as compared to arc discharge. The transition to arc mode results in smaller kernels than expected with smaller total energy. By looking at the uncorrected energy data in Fig. 10b, we know that the results do not consider only thermal energy with the assumption that the total volume of the kernel should be proportional to the thermal energy. The final volume of the 12<sup>th</sup> kernel (counting images in Fig. 10a from left to right and top to bottom) shows a smaller kernel than the 11<sup>th</sup> test. The original energy that includes cathode fall suggest that this volume should be the largest, however, by removing the cathode fall, the trend shown in the energy is more proportional to the final volume resulting in a better prediction of relative kernel size.



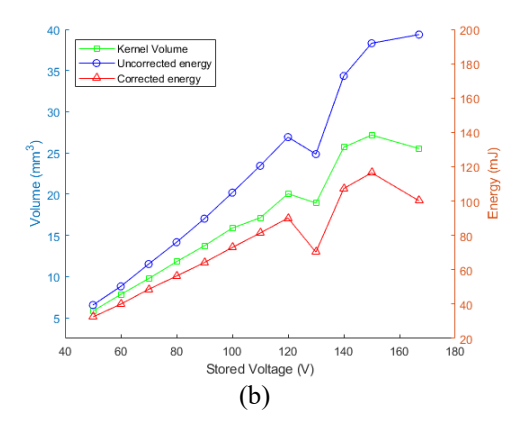


**FIGURE 10:** (a) KERNEL IMAGES DURING PURE GLOW DISCHARGE (TOP TWO ROWS) AND AT END OF DISCHARGE (BOTTOM TWO ROWS) AND (b) PLOT OF FINAL VOLUME AND FINAL ENERGY.

## 4. CONCLUSION

The work explores how electrical energy is dissipated within the plasma event and several conclusions and insights about both the voltage measurement and the structure of the plasma are reached and summarize here.

- 1. The zero-length extrapolation or gap change method appears to measure both cathode and anode fall without distinguishing between the two.
- 2. Simply measuring the voltage of the plasma with a probe appears to give a comparable cathode fall measurement for this pressure and condition when compared to the zero-length extrapolation method. Utilizing an intrusive probe in this manner should be done with careful analysis as the probe has the potential to greatly affect the measured values. The effect of the probe and affects from plasma on the measurement is considered to be small for this work and this point is discussed in more detail in the next paragraph
- 3. The surface condition of the electrode is just as important as the material and gas composition for the measurement and production of glow discharge. The electric field can be greatly affected by geometry such as sharp or rough edges. Changing electric field at the surface will affect the physical formation and voltage requirements of the sheath.
- 4. The glow discharge is axially symmetric about the cathode. After examining literature and schlieren images shown in this work it is found that glow discharge plasma encompasses the entire circumference of the high electrode cylindrical tip which is beneficial for size measurement of the ignition kernels. The surface area of the arc plasma on the electrode is reduced to a small spot greatly changing the geometry depending on the location and duration of the discharge.
- 5. The current density requirement for glow discharge follows the literature (as discussed with Eqn. 2) even at

these elevated pressures. Early experiments with glow plasma generally utilize low pressure gas tubes to maintain a steady discharge over time which makes the relationship between current and surface area of glow discharge (constant current density) easy to experimentally observe. The preliminary work provided here shows that there is a constant current density however this work does not evaluate a value at these pressures.

6. For finely polished (10k grit sandpaper) stainless steel electrodes in dry atmospheric pressure air the cathode fall was found to be approximately 330V, but this should be measured case by case if needed since the value is sensitive to electrode condition.

The two viable methods for measuring cathode fall presented, give similar measurements for the magnitude of the total potential drop across the cathode and anode sheath. The major difference between these two methods is the addition differentiation between anode and cathode sheath voltage drops for the intrusive method. The distinction between the two sheaths is desired for future work, because, for the DC case, the weak electric field that produces the anode sheath may not result in non-thermal energy if the thickness of the sheath is significantly larger than the cathode sheath (produced by the strong electric field at the cathode).

Additional comment should be made in regard to the probe measurement. The initial issue with direct measurement of the plasma comes from the presence of positive ions in the plasma; however, at these pressures and current densities, the charge measurement at the probe surface is less controlled by the field effects that produce sheaths and more by the rate of collisions with the probe. Since the density of highly energetic electrons is much greater than the heavy ionized particles, we can consider the charge measured to be mainly from the bombardment of electrons. The bombardment of electrons as the current passes through the probe will help prevent a sheath or positive charge from building on the probe surface. This assumption is supported by the consistent measurement between the two methods where the difference between the measurement of the two tests is too small to conclude if the difference is from positive ions present in the plasma or experimental uncertainty and error.

Removing the energy dissipated across the cathode fall should represent the thermal energy of the spark and this is suggested through the energy and kernel volume analysis however further examination of arc discharge is needed. Further experimental validation for assessing the measured thermal energy could be found by measuring the thermal losses via calorimetry such as in Kim [21] which would determine if other losses such as conduction to the electrode are significant. In a separate work the value of the cathode fall found is used in a thermodynamic model to predict the kernel volume over the duration of the spark

## **ACKNOWLEDGEMENTS**

This material is based upon work supported by the National Science Foundation (NSF) under Federal Award No. CBET-2039486 issued through Combustion and Fire System (CFS) program.

#### **REFERENCES**

- [1] Langmuir, I., 1923, "Positive Ion Currents from the Positive Column of Mercury Arcs," Science (80-.)., 58(1502), pp. 290–291. DOI 10.1126/science.58.1502.290.
- [2] Tonks, L., and Langmuir, I., 1929, "A General Theory of the Plasma of an Arc," Phys. Rev., **34**(6), pp. 876–922. DOI 10.1103/PhysRev.34.876.
- [3] Lieberman, M. A., and Lichtenberg, A. J., 2005, Principles of Plasma Discharges and Materials Processing: Second Edition, John Wiley & Sons, Inc., Hoboken, NJ, USA.
- [4] Venkattraman, A., 2013, "Cathode Fall Model and Current-Voltage Characteristics of Field Emission Driven Direct Current Microplasmas," Phys. Plasmas, **20**(11), p. 113505. DOI 10.1063/1.4829680.
- [5] Prevosto, L., Kelly, H., Mancinelli, B., Chamorro, J. C., and Cejas, E., 2015, "On the Physical Processes Ruling an Atmospheric Pressure Air Glow Discharge Operating in an Intermediate Current Regime," Phys. Plasmas, 22(2). DOI 10.1063/1.4907661.
- [6] Gadri, R. B., 1999, "One Atmosphere Glow Discharge Structure Revealed by Computer Modeling," IEEE Trans. Plasma Sci., **27**(1), pp. 36–37. DOI 10.1109/27.763018.
- [7] Kolobov, V. I., and Tsendin, L. D., 1992, "Analytic Model of the Cathode Region of a Short Glow Discharge in Light Gases," Phys. Rev. A, **46**(12), pp. 7837–7852. DOI 10.1103/PhysRevA.46.7837.
- [8] Sommerer, T. J., Hitchon, W. N. G., and Lawler, J. E., 1989, "Self-Consistent Kinetic Model of the Cathode Fall of a Glow Discharge," Phys. Rev. A, **39**(12), pp. 6356–6366. DOI 10.1103/PhysRevA.39.6356.
- [9] Staack, D., Farouk, B., Gutsol, A., and Fridman, A., 2008, "DC Normal Glow Discharges in Atmospheric Pressure Atomic and Molecular Gases," Plasma Sources Sci. Technol., 17(2), p. 25013. DOI 10.1088/0963-0252/17/2/025013.
- [10] Shi, J. J., and Kong, M. G., 2003, "Cathode Fall Characteristics in a Dc Atmospheric Pressure Glow Discharge," J. Appl. Phys., **94**(9), pp. 5504–5513. DOI 10.1063/1.1615296.
- [11] Arkhipenko, V. I., Kirillov, A. A., Safronau, Y. A.,

- Simonchik, L. V., and Zgirouski, S. M., 2012, "Plasma Non-Equilibrium of the DC Normal Glow Discharges in Atmospheric Pressure Atomic and Molecular Gases," Eur. Phys. J. D, **66**(10), p. 252. DOI 10.1140/epid/e2012-30359-x.
- [12] Benilov, M. S., Benilova, L. G., Li, H. P., and Wu, G. Q., 2012, "Sheath and Arc-Column Voltages in High-Pressure Arc Discharges," J. Phys. D. Appl. Phys., 45(35), p. 10. DOI 10.1088/0022-3727/45/35/355201.
- [13] Uhrlandt, D., Baeva, M., Pipa, A. V., Kozakov, R., and Gött, G., 2015, "Cathode Fall Voltage of TIG Arcs from a Non-Equilibrium Arc Model," Weld. World, **59**(1), pp. 127–135. DOI 10.1007/s40194-014-0188-x.
- [14] Lichtenberg, S., Dabringhausen, L., Langenscheidt, O., and Mentel, J., 2005, "The Plasma Boundary Layer of HID-Cathodes: Modelling and Numerical Results," *Journal of Physics D: Applied Physics*, pp. 3112–3127.
- [15] Luhmann, J., Lichtenberg, S., Langenscheidt, O., Benilov, M. S., and Mentel, J., 2002, "Determination of HID Electrode Falls in a Model Lamp II: Langmuir-Probe Measurements," J. Phys. D. Appl. Phys., **35**(14), pp. 1631–1638. DOI 10.1088/0022-3727/35/14/303.
- [16] Ziegler, G. F. W., Wagner, E. P., and Maly, R. R., 1985, "Ignition of Lean Methane-Air Mixtures by High Pressure Glow and ARC Discharges," Symp. Combust., 20(1), pp. 1817–1824. DOI 10.1016/S0082-0784(85)80679-2.
- [17] Cobine, J. D., 1942, "Gaseous Conductors, Theory and Engineering Applications," J. Franklin Inst., **233**(3), p. 292. DOI 10.1016/s0016-0032(42)90330-2.
- [18] Hao, Y., Zheng, B., and Liu, Y., 2013, "Cathode Fall Measurement in a Dielectric Barrier Discharge in Helium," Phys. Plasmas, **20**(11). DOI 10.1063/1.4834515.
- [19] "US4733646A Automotive Ignition Systems Google Patents" [Online]. Available: https://patents.google.com/patent/US4733646A/en. [Accessed: 15-Mar-2021].
- [20] Billoux, T., Cressault, Y., Teulet, P., and Gleizes, A., 2012, "Calculation of the Net Emission Coefficient of an Air Thermal Plasma at Very High Pressure," *Journal of Physics: Conference Series*.
- [21] Kim, K., Hall, M. J., Wilson, P. S., and Matthews, R. D., 2020, "Arc-Phase Spark Plug Energy Deposition Characteristics Measured Using a Spark Plug Calorimeter Based on Differential Pressure Measurement," Energies, 13(14). DOI 10.3390/en13143550.